

$^{30}\text{Si} + ^{14}\text{N}$ radiative capture*A. F. Zeller,[†] H. S. Plendl, R. H. Davis, M. E. Williams,[‡] and C. I. Delaune[§]*Department of Physics, The Florida State University, Tallahassee, Florida 32306*R. Holub^{||}*Department of Chemistry, The Florida State University, Tallahassee, Florida 32306*

(Received 18 February 1975)

Cross sections for the reactions $^{30}\text{Si}(^{14}\text{N},\gamma)^{44}\text{Sc}^m$ and $^{30}\text{Si}(^{14}\text{N},n)^{43}\text{Sc}$ have been measured at five bombarding energies in the 40 to 62 MeV range. Residual activities produced by the reactions are unique and sufficiently long-lived so that the reaction yields in thick targets of natural Si were measured off-line with a Ge(Li) detector. By unfolding the range-energy function, the cross sections were extracted from the yields. The capture cross section increases from 7.5 to 22 μb over the bombarding energy range. The cross section for single neutron emission is 75 μb and constant within the errors of this experiment. A Blann-Plasil code calculation resulted in a value that is a factor of 10^3 lower. The experimental results have been analyzed to determine an upper limit on the moment of inertia of the excited compound nucleus. Values of the upper limit depend on the choice of optical model parameters and the radius parameter in the moment of inertia.

NUCLEAR REACTIONS $^{30}\text{Si} + ^{14}\text{N}$, $E = 40\text{--}62$ MeV; measured yields of activation products ^{43}Sc and $^{44}\text{Sc}^m$; calculated cross sections and limits on the moments of inertia. Natural targets, Ge(Li) detector.

I. INTRODUCTION

The cross section for radiative capture of heavy ions is small compared to the total reaction cross section, since most of the absorption of incoming partial waves is the result of fusion-evaporation or direct reaction processes or both. Even if the compound nucleus formation cross section is large, the fused system with initial excitation energy E_0^* will energetically relax by particle emission until the energy of the nucleus falls to a value $(E_{\text{yrast}} + B_n)$, where E_{yrast} is the rotational energy for a given angular momentum and B_n is the nucleon binding energy. This is illustrated in the upper part of Fig. 1, where particle emission is allowed in region 1, for which $E^* > (E_{\text{yrast}} + B_n)$. Passage through region 2 is via γ -ray decay, since at $E^* = (E_{\text{yrast}} + B_n)$ the probability for γ -ray emission¹ is approximately 50%, while at $E^* < (E_{\text{yrast}} + B_n)$ there is insufficient energy for further particle emission. As shown in the lower part of Fig. 1, most of the cross section for both compound nucleus formation (region 3) and any direct processes (region 4) lies below the angular momentum J' for which $E_0^* = (E_{\text{yrast}} + B_n)$.

Radiative decay with no particle emission becomes the dominant mode for compound nucleus relaxation for $J > J'$ (and E^* less than the fission barrier). The concentration of radiative capture strength in the tail of the partial cross-section distribution (shaded area of Fig. 1) spans a relatively narrow interval of J values of the compound

system and a correspondingly small interval of partial wave angular momenta Δl . A measurement of the radiative capture cross section is of interest because it directly measures the high- l tail for compound nucleus formation. Furthermore, if J' is estimated, the intercept $E_0^* = E_{\text{yrast}} + B_n$ is determined by definition, and from this the moment of inertia can be established, since

$$E_{\text{yrast}} = \frac{\hbar^2}{2I} J'(J'+1), \quad (1)$$

and E_0^* and B_n are known.

The value of J' is fixed by finding the lower truncation J value such that the computed cross section for $J \geq J'$ is equal to the measured value. As discussed in Sec. IV, this procedure is reaction model dependent. Further, an unmeasured fraction of the total reaction cross section, the tail of region 4 in Fig. 1 which extends above J' , is due to direct reaction processes. As a result, the value of the moment of inertia obtained from Eq. (1) is an upper bound.

While the radiative capture of light particles has been extensively studied for years, little work has been done on the radiative capture of heavy ions. The few previous experiments are characterized by results with large uncertainties. The ^{16}O bombardment of ^{27}Al and ^{31}P by Coleman, Herbert, and Perkin² placed upper limits of 0.27 and 18 μb , respectively, on the radiative capture cross sections. The ^{13}C bombardment of ^{19}F by Fremlin and Reasbeck³ gave uncertain results because of

impurities in the target. Linder and Zucker⁴ studied the $^{31}\text{P}(^{14}\text{N}, \gamma)$ reaction, but the poor nature of phosphorus targets and high background gave unreliable results. Observations of high energy γ rays (>10 MeV) were attempted by Carlson and Throop⁵ and by Feldman and Heikkinen,⁶ and the latter attributed the high energy γ -ray yield to the radiative capture process.

Since very small cross sections are expected, a high-efficiency detection technique is necessary. The off-line measurement of γ rays from radioactive residual nuclei produced by the reaction in thick targets is advantageous, but this technique places several stringent conditions on the design of the experiment: (1) The decay of the compound nucleus must produce a γ ray which is well isolated in energy; (2) the lifetime must be sufficiently long to make off-line measurement practical; and (3) because of inevitable trace contamination by C, O, and Si, the target must have $Z \geq 14$.

The system $^{30}\text{Si} + ^{14}\text{N}$ satisfies these requirements. Because of the possible contributions

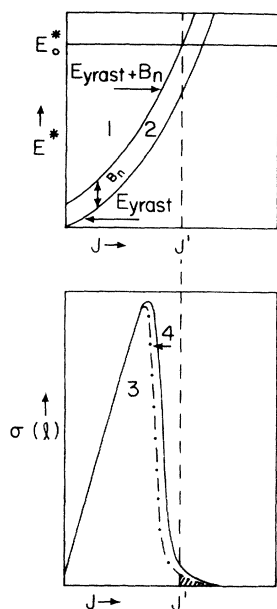


FIG. 1. Schematic plot of excitation energy E^* versus spin J showing the yrast line and the curve that is displaced from the yrast line by the binding energy of the neutron B_n . E_0^* is the initial excitation energy of the system, and J' is the spin for which $E_0^* = E_{\text{yrast}} + B_n$. Region 1 decays predominantly by particle emission, region 2 by γ emission. The solid line in the lower part of the figure is a typical spin distribution in σ vs J space. Region 3 corresponds to complete fusion, region 4 to direct reactions. The dot-dashed line indicates the decrease in formation of high-spin states due to direct reactions. The shaded portion is the region corresponding to radiative capture.

from the $(^{14}\text{N}, xn)$ reactions on other Si isotopes, only ^{30}Si was considered. In addition to the $^{30}\text{Si}(^{14}\text{N}, \gamma)^{44}\text{Sc}^m$ reaction, the $^{30}\text{Si}(^{14}\text{N}, n)^{43}\text{Sc}$ reaction has also been observed. The pertinent decay characteristics of the reaction products are listed in Table I. Preliminary results of this work have been reported elsewhere.⁸

II. EXPERIMENTAL PROCEDURE

A beam of NH_2^- ions from the Heinicke direct extraction source⁹ was accelerated in the Florida State University super FN tandem and was foil stripped in the terminal. The +5 or +6 beams were again accelerated to energies in the range from 40 to 62 MeV. Thick targets were made of natural, hyperpure Si crystals (largest contamination: <0.5 parts/ 10^9 phosphorus), and the surfaces were thoroughly cleaned. Irradiation times were 6–14 h, and beam currents ranged from 50 to 150 nA. Special care to prevent contamination from K, Cl, and P was taken.

After irradiation, the targets were counted with a shielded, off-line 20 cm³ Ge(Li) detector system which had a resolution of 2.3 keV at $E_\gamma = 1.33$ MeV. The detector was calibrated for energy and efficiency with standard sources. After several hours, during which the shorter-lived activities consisting mainly of ^{38}K , ^{34}Cl , and other β^+ emitters decayed, the targets were counted for 100 minutes. The counting time was increased to 1500 minutes after a few days and counting was continued for two weeks. Figures 2 and 3 show the low-energy portion of a typical spectrum. In Fig. 2, the high pair-annihilation background in the region of interest is evident. In Fig. 3, the 511 keV peak is considerably decreased and the 477 keV photopeak from the decay of ^7Be ($T_{1/2} = 53.5$ day) is observed. The yields for ^7Be were calculated and served as an internal check on integration by comparison with previously determined ^7Be excitation functions.¹⁰ No γ rays corresponding to the decay of products with $Z > 21$ were observed.

TABLE I. Decay characteristics of product nuclei (Ref. 7).

Nuclide	$T_{1/2}$ (h)	E_γ (keV)	Branching ratio or relative intensity
^{43}Sc	3.891	373	25%
$^{44}\text{Sc}^g$	3.927	1157	99%
$^{44}\text{Sc}^m$	58.6	271	99
		1157	98

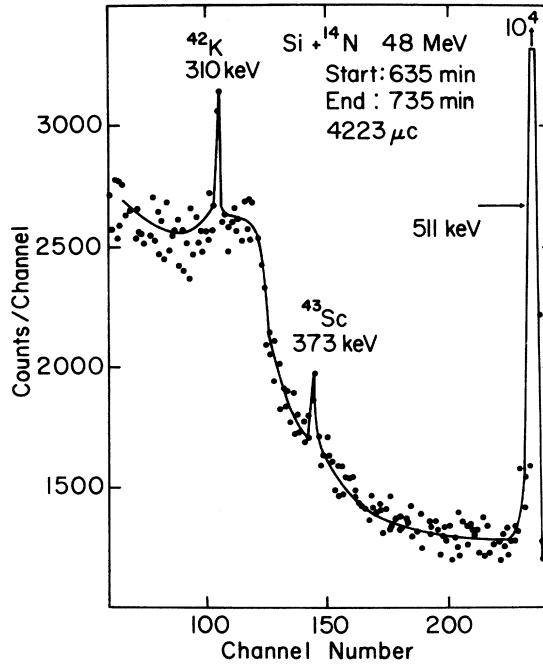


FIG. 2. Typical γ -ray spectrum showing the low-energy end of the spectrum taken shortly after the end of bombardment.

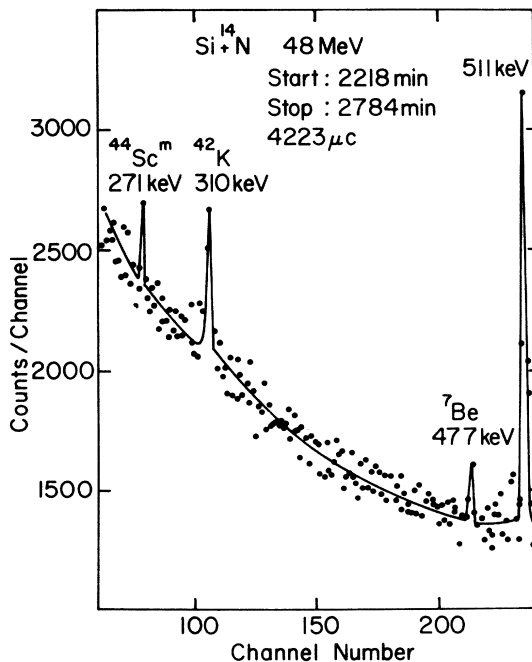


FIG. 3. Typical γ -ray spectrum showing the low-energy end after the short-lived activities have died away.

III. RESULTS

Yield curves for $^{30}\text{Si}(^{14}\text{N}, \gamma)^{44}\text{Sc}^m$ and $^{30}\text{Si}(^{14}\text{N}, n)^{43}\text{Sc}$ reactions are shown in Fig. 4. The error bars represent uncertainties due to counting statistics only. Other errors (integration, background subtraction, efficiency calibration, and branching ratios) contribute an additional estimated 10% error. The solid line is an empirical representation of the data.

Cross sections were calculated from the yield curves by the relation

$$\sigma = \frac{\Delta Y}{\Delta R}, \quad (2)$$

where ΔY is the difference in the yield for an energy interval and ΔR is the range¹¹ difference in that interval. The use of thick targets in this experiment has the advantage of smoothing over any fluctuations in the compound nucleus formation cross section.¹² The cross sections for ^{43}Sc and $^{44}\text{Sc}^m$ are shown in Fig. 5. For comparison of the relative energy dependence of the data with that for the total reaction cross section σ_R , the latter is shown as a solid line arbitrarily normalized downward by a factor of approximately 10^{-5} . The optical model code JIB¹³ was used to calculate σ_R . Absolute errors in the $^{44}\text{Sc}^m$ cross sections range from 45% at the lowest energies to 20% at the highest. The ^{43}Sc cross-section errors are estimated to be 40% throughout.

Because of the high background (as seen in Fig. 2), the yields for $^{44}\text{Sc}^e$ decay could not be extracted. The decay of the $^{44}\text{Sc}^m$ is taken as a measure of the radiative capture yield, since the contribu-

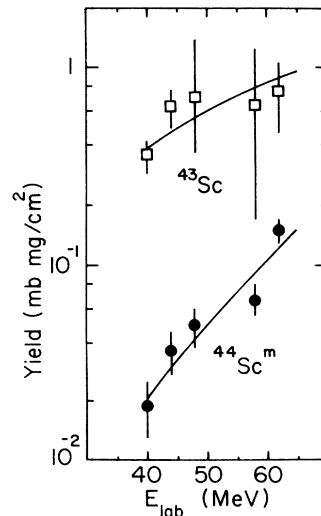


FIG. 4. Experimental yield curves for $^{30}\text{Si}(^{14}\text{N}, n)^{43}\text{Sc}$ and $^{30}\text{Si}(^{14}\text{N}, \gamma)^{44}\text{Sc}^m$. Error bars represent counting statistics.

tion from the ground state decay is expected to be small. For a statistical process at high energy, the ratio of the yields depends on $2J+1$, which provides a strong preference for population of the $J=6^+$ metastable state compared to the $J=2^+$ ground state.⁷ Thus the expected ratio of isomeric to ground-state contribution to the radiative capture cross section is of the order of 13:5. Williams and Toth¹⁴ found these ratios for $^{31}\text{P}(^{14}\text{N}, p)^{44}\text{Sc}$ and $^{32}\text{Sc}(^{14}\text{N}, p)^{44}\text{Sc}$ to be 9:1 and 7:1, respectively, at 42 MeV.

There is a possible spurious contribution to the $^{30}\text{Si}(^{14}\text{N}, n)^{43}\text{Sc}$ yield from the reaction $^{29}\text{Si}(^{14}\text{N}, \gamma)^{43}\text{Sc}$. The results of the present experiment support the assumption that the cross section for radiative capture is small ($\leq 10\%$) compared to the single neutron emission cross section; hence, the contribution due to the $^{29}\text{Si}(^{14}\text{N}, \gamma)^{43}\text{Sc}$ reaction has been neglected.

IV. DISCUSSION

In Fig. 5, it is seen that the experimental radiative capture cross section increases with bombarding energy more rapidly than the calculated total reaction cross section. In the lower part of Fig. 1, the radiative capture cross section is represented by the shaded area. As the energy is increased, the shaded area moves up in J as higher-order transmission coefficients become significant, while at the same time the J value for neutron emission (J') moves up. The cross-section change with energy is sensitive to the difference between the addition of new partial-wave contri-

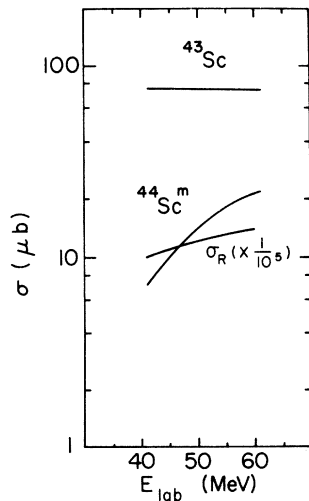


FIG. 5. Excitation function for $^{30}\text{Si}(^{14}\text{N}, n)^{43}\text{Sc}$ and $^{30}\text{Si}(^{14}\text{N}, \gamma)^{44}\text{Sc}^m$. The calculated total reaction cross section σ_R as shown has to be multiplied by 10^5 .

butions as l grazing increases and the deletion of low partial-wave contributions as single neutron evaporation opens. A complete calculation must take into account the details of the barrier, the probability of compound nucleus formation, and the probability of purely γ -ray decay; but it can be readily shown that the J interval for radiative capture ($J_g - J'$), where J_g is the grazing angular momentum value, increases as the bombarding energy increases.

To show that $(J_g - J')$ increases with energy, it is sufficient to show that

$$\frac{dJ'}{dE} / \frac{dJ_g}{dE} < 1. \quad (3)$$

From Fig. 1 and Eq. (1),

$$E^* - B_n = E + Q - B_n = \frac{\hbar^2}{2I} J'(J'+1) \approx \frac{\hbar^2}{2I} J'^2 \quad (4)$$

for large J' . Here Q is the Q value for compound nucleus formation and E is the bombarding energy. Solving for J' yields

$$J' = \left(\frac{2I}{\hbar^2} \right)^{1/2} (E + Q - B_n)^{1/2}. \quad (5)$$

The rotational energy of the system formed in a grazing collision with angular momentum J_g is given by

$$E_{\text{rot}} + E - V_0 = \frac{\hbar^2}{2I_g} J_g(J_g + 1) \approx \frac{\hbar^2}{2I_g} J_g^2 \quad (6)$$

for large J_g . The quantity I_g is the moment of inertia formed by the reactant nuclei in contact, and V_0 is the barrier for $l=0$. Solving Eq. (6) for J_g ,

$$J_g = \left(\frac{2I_g}{\hbar^2} \right)^{1/2} (E - V_0)^{1/2}. \quad (7)$$

After taking derivatives of J' and J_g with respect to E , the center of mass energy, the left-hand side of Eq. (3) is given by

$$\frac{dJ'}{dE} / \frac{dJ_g}{dE} = \left(\frac{I}{I_g} \right)^{1/2} \left(\frac{E - V_0}{E + Q - B_n} \right)^{1/2}. \quad (8)$$

The ratio I/I_g is bound by $I/I_g \leq 1$, since the deformation at grazing is equal or greater than that of the compound nucleus. Letting $I/I_g = 1$ and using the values $V_0 = 15.2$ MeV, $Q = +16.3$ MeV, and $B_n = 9.7$ MeV,

$$\begin{aligned} \frac{dJ'}{dE} / \frac{dJ_g}{dE} &= 1 \times \left(\frac{E - 15.2}{E + 16.3 - 9.7} \right)^{1/2} \\ &= \left(\frac{E - 15.2}{E + 6.6} \right)^{1/2} < 1. \end{aligned} \quad (9)$$

The cross section for single neutron emission $^{30}\text{Si}(^{14}\text{N}, n)^{43}\text{Sc}$ is 75 μb and constant as a function

of beam energy within the uncertainties of the experiment (Fig. 5). This result is provocative in that a calculation of the cross section for this process at 50 MeV by the evaporation code developed by Blann and Plasil¹⁵ results in a value of 86 mb, i.e., a value that is a factor of 10^3 higher than the experimental value. One-neutron evaporation is preferentially fed by high- J states, since for J values lower than the value needed for two-neutron evaporation [i.e., the intercept J value for $(E_{\text{yrast}} + B_n + B'_n) = E_0^*$ in Fig. 1] multinucleon decay effectively competes.

There are two possible explanations for the large discrepancy between experimental and calculated single-neutron emission cross sections: (a) High- J state formation is suppressed with respect to the mechanisms assumed in the code, i.e., a large part of the total reaction cross section for high- J values is due to direct processes; this would yield inordinately large transmission coefficients in optical model analyses, and such transmission coefficients are used in the code. (b) The treatment of angular momentum restriction in the code is inadequate. The consequences of (a) will become apparent in the discussion of the moment of inertia. The effects of the s -wave approximation and of other simplifications used in the Blann-Plasil approach have been noted previously.¹⁰

An upper limit can be placed on J' and through it an upper limit on the moment of inertia. The total reaction cross section is given by the sum of the partial cross sections

$$\sigma_R = \pi\lambda^2 \sum_{l=0}^{\infty} (2l+1)T_l, \quad (10)$$

where the transmission coefficients T_l are determined from optical model or parabolic barrier model fits to scattering data. If the fusion cross section dominated the reaction process, then the capture cross section would be given by

$$\sigma_{\text{capture}} = \pi\lambda^2 \sum_{l>J'}^{\infty} (2l+1)T_l, \quad (11)$$

where J' corresponds to the intercept of the $(E_{\text{yrast}} + B_n)$ line (the 50% γ -emission line) with E_0^* . Since J' is a fitting parameter in Eq. (11) and the

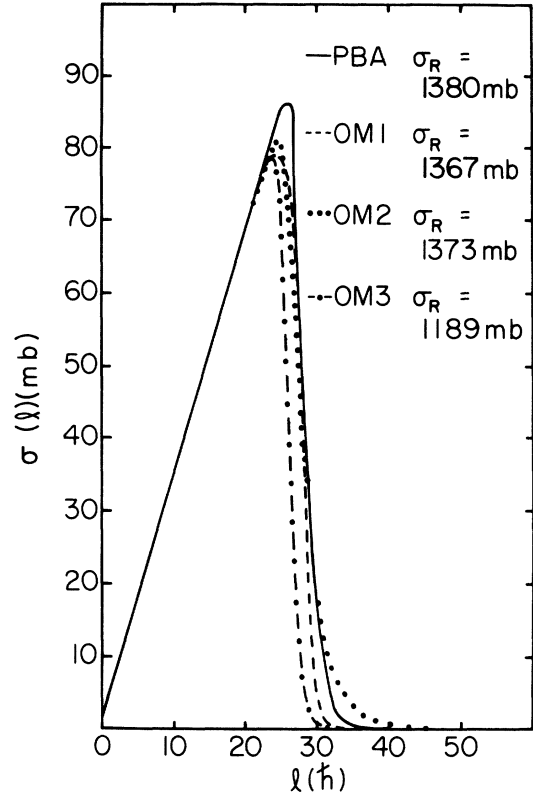


FIG. 6. $\sigma(l)$ plotted as a function of l for $^{30}\text{Si} + ^{14}\text{N}$ at 60 MeV using the PBA and several optical model parameter sets.

capture cross section is measured, the resulting J' value determines the moment of inertia.

The $(E_{\text{yrast}} + B_n)$ line which determines J' can be understood as the value of J for which particle emission becomes possible, since the available energy E_a equals B_n . One would expect that particle emission has a 100% probability when $E_a > B_n$ and zero probability when $E_a < B_n$. However, because of barrier penetration, the probability of particle emission at the $(E_{\text{yrast}} + B_n)$ line is 50%, and so is the probability of γ -ray emission (with a width of the order of a few hundred keV).¹ In the determination of the moment of inertia, the actual probability is not critical, since a change of $\pm 1\hbar$ in J' would change the calculated cross section by

TABLE II. Optical model parameter sets.

Set	U (MeV)	R_r (fm) ^a	a_r (fm)	W_S (MeV)	R_i (fm) ^a	a_i (fm)	System	E_{lab} (MeV)	Ref.
OM1	100	0.85	0.84	8	1.48	0.18	$^{12}\text{C}(^{14}\text{N}, ^{14}\text{N})^{12}\text{C}$	78	17
OM2	16.1	1.3	0.6	4.1	1.3	0.6	$^{40}\text{Ca}(^{14}\text{N}, ^{14}\text{N})^{40}\text{Ca}$	36	18
OM3	17	1.306	0.42	12.48	1.24	0.25	$^{26}\text{Mg}(^{16}\text{O}, ^{16}\text{O})^{26}\text{Mg}$	50	19

^a Radii defined by $R_{\text{real}} = R_r(A_{\text{tar}}^{1/3} + A_{\text{proj}}^{1/3})$ and $R_{\text{im}} = R_i(A_{\text{tar}}^{1/3} + A_{\text{proj}}^{1/3})$.

TABLE III. Moments of inertia from the parabolic barrier approximation (PBA) and the optical model parameter sets.

E_{lab}	Set	J' (\hbar)	$I/I_{\text{rig}}(1.0 \text{ fm})$	$I/I_{\text{rig}}(1.17 \text{ fm})$	$I/I_{\text{rig}}(1.4 \text{ fm})$
40	PBA	27	0.81 ± 0.06	0.59 ± 0.04	0.41 ± 0.03
	OM1	28	0.87 ± 0.07	0.63 ± 0.04	0.44 ± 0.03
	OM2	35	1.34 ± 0.07	0.98 ± 0.05	0.69 ± 0.04
50	OM3	25	0.69 ± 0.05	0.51 ± 0.04	0.35 ± 0.02
	PBA	30	0.83 ± 0.06	0.61 ± 0.04	0.42 ± 0.02
	OM1	33	1.00 ± 0.07	0.73 ± 0.05	0.51 ± 0.04
60	OM2	41	1.54 ± 0.08	1.12 ± 0.05	0.78 ± 0.04
	OM3	29	0.78 ± 0.05	0.57 ± 0.04	0.40 ± 0.02
	PBA	33	0.86 ± 0.06	0.63 ± 0.04	0.44 ± 0.03
	OM1	37	1.08 ± 0.07	0.79 ± 0.05	0.55 ± 0.04
	OM2	46	1.66 ± 0.08	1.21 ± 0.05	0.85 ± 0.04
	OM3	33	0.86 ± 0.06	0.63 ± 0.04	0.44 ± 0.03

a factor of 4. The moment of inertia is, therefore, well determined to within the uncertainties in optical model parameters and in the radius parameter r_0 .

The partial cross sections $\sigma(l)$ used in the upper limit calculation are shown in Fig. 6 as a function of l . The parabolic barrier approximation model is that of Thomas,¹⁶ and the optical model parameters, as listed in Table II, are obtained from elastic scattering as reported in the literature.¹⁷⁻¹⁹

The upper limits for the ratio of the moment of inertia to the rigid body value resulting from the analysis are given in Table III. The results are given in terms of the J' values corresponding to several barrier models and the r_0 values used in the calculation of the rigid body value of the moment of inertia,

$$I_{\text{rig}} = \frac{2}{5} mR^2, \quad (12)$$

where $R = r_0 A^{1/3}$. The r_0 values used in that calculation were 1.17 fm (suggested by Thomas¹⁶), 1.4 fm, and 1.0 fm (Bass²⁰). The variation in the values obtained for the moment of inertia ratio from the several barrier models points out the need for improved optical model potentials for heavy ion reactions.

The competition for high partial waves among direct processes, fission, single and multiple neu-

tron emission, and charged particle emission has the effect of decreasing the value of J' and, hence, of I . Since in determining the upper limit for I it was assumed that $\sigma_{\text{com.nuc.}} = \sigma_R$, the opening of any competing channel that results in $\sigma_{\text{com.nuc.}} < \sigma_R$ requires a smaller value of J' to conserve the magnitude of the radiative capture cross section. Clearly, the use of any model which abruptly cuts off the compound nucleus cross section below l_{grazing} leads to a smaller value of I .

It is apparent that more work at higher incident energies is necessary to determine the extent of the trend towards larger values of I with increasing incident energy that has been noted both in the present work and in previous work on $^{12}\text{C} + ^{14}\text{N}$ by Stokstad.²¹ Experimental determinations of σ_R and of σ_{direct} values for the $^{30}\text{Si} + ^{14}\text{N}$ system would make it possible to place more definite limits on I than could be done in the absence of such values.

ACKNOWLEDGMENTS

We acknowledge the participation of R. J. de Meijer in the preliminary stages of the work and the assistance in data collection of G. KeKelis and R. Eaker. Two of us (AFZ and RH) wish to acknowledge the support of G. R. Choppin in the early stages of this work.

*Research supported in part by the National Science Foundation under Grants Nos. NSF-GU-2612 and NSF-GP-25974.

† Also supported by U.S. Atomic Energy Commission Grant No. AT (40-1) 1797. Present address: Department of Nuclear Physics, The Australian National University, Box 4, Canberra, A.C.T., Australia 2600.

‡ Present address: Physics Department, Ripon College, Ripon, Wisconsin 54971.

§ Present address: IN-CSD 5A, John F. Kennedy Space Center, Kennedy Space Center, Florida 32899.

|| Supported in part by U.S. Atomic Energy Commission Grant No. AT (40-1) 1797. Present address: U.S. Bureau of Mines, Building 20, Denver Federal Center, Denver, Colorado 80225.

¹J. R. Grover and J. Gilat, Phys. Rev. 157, 804, 814 (1967).

²R. F. Coleman, D. N. Herbert, and J. L. Perkin, Proc.

- Phys. Soc. London 77, 526 (1961).
- ³J. H. Fremlin and P. Reasbeck, Proc. Phys. Soc. London 82, 110 (1963).
- ⁴B. Linder and A. Zucker, Phys. Rev. 127, 1280 (1962).
- ⁵R. R. Carlson and M. J. Throop, Phys. Rev. 136, B630 (1964).
- ⁶W. Feldman and D. W. Heikkinen, Nucl. Phys. A133, 177 (1969).
- ⁷P. M. Endt and C. Van der Leun, Nucl. Phys. A214, 1 (1973).
- ⁸A. F. Zeller, H. S. Plendl, R. H. Davis, M. E. Williams, and C. I. Delaune, Bull. Am. Phys. Soc. 19, 990 (1974).
- ⁹E. Heinicke, K. Bethge, and H. Baumann, Nucl. Instrum. Methods 58, 125 (1968).
- ¹⁰R. Holub, A. F. Zeller, H. S. Plendl, and R. J. de Meijer, Nucl. Phys. A246, 515 (1975).
- ¹¹L. C. Northcliffe and R. F. Schilling, Nucl. Data A7, 233 (1970).
- ¹²T. Ericson, Adv. Phys. 9, 425 (1960).
- ¹³F. G. Perey, Phys. Rev. 131, 745 (1963).
- ¹⁴I. R. Williams and K. S. Toth, Phys. Rev. 138, B382 (1965).
- ¹⁵M. Blann and F. Plasil, Phys. Rev. Lett. 29, 303 (1972).
- ¹⁶T. D. Thomas, Phys. Rev. 116, 703 (1959).
- ¹⁷W. Von Oertzen, M. Liu, C. Caverzasio, J. C. Jacmart, F. Pougheon, M. Riou, J. C. Raynette, and C. Stephan, Nucl. Phys. A143, 34 (1970).
- ¹⁸M. E. Williams, R. H. Davis, C. I. Delaune, G. M. Hudson, K. W. Kemper, and A. F. Zeller, Phys. Rev. C 11, 906 (1975).
- ¹⁹R. H. Siemssen, H. T. Fortune, A. Richter, and J. L. Yntema, in *Proceedings of the International Conference on Nuclear Reactions Induced by Heavy Ions, Heidelberg, Germany, July 1969*, edited by R. Bock and W. R. Hering (North-Holland, Amsterdam, 1970), p. 72.
- ²⁰R. Bass, Phys. Lett. 47B, 139 (1973).
- ²¹R. G. Stokstad, in *Proceedings of the International Conference on Reactions between Complex Nuclei, Nashville, Tennessee, June 1974*, edited by R. L. Robinson, F. K. McGowan, J. B. Ball, and J. H. Hamilton (North-Holland, Amsterdam/American Elsevier, New York, 1974), p. 327.